Check for updates

Batteries & Supercaps

Research Article
doi.org/10.1002/batt.202300225

Chemistry Europe
European Chemical Societies Publishing

www.batteries-supercaps.org

Investigations into Improved Electrochemical Performance of Sn Doped Hard Carbons as Negatives for Sodium-Ion Batteries

Abhinav Tripathi,[a, b] Chinnasamy Murugesan,[a, b] Aaron Naden,[a, b] Peter Curran,[c] Chris M. Kavanagh,[c] James M. Condliffe,[d] A. Robert Armstrong,[a, b] and John T. S. Irvine*[a, b]

Hard carbons are the most suitable anode materials for practical sodium-ion batteries (NIBs). Despite various studies, there is still significant scope for improvement in the understanding of the (de)sodiation mechanisms. Here, we study Sn incorporation in waste derived commercial and model sucrose derived hard carbons and its effect on the electrochemical performance. Sn incorporation leads to improved first cycle coulombic efficiency and capacity, specifically increase in the plateau capacity. An improvement from 220 mAh/g to 285 mAh/g and 325 mAh/g is respectively obtained for 7% and 15% Sn in hard carbon-Sn composites (HC/Sn). Sn incorporation in both hard carbons has been shown to improve the electrochemical performance, notably achieving a synergy with capacities in excess of that expected from simple addition. For example, 7% Sn additions tend to increase capacity by 25%, twice that predicted from simple addition. X-ray diffraction (XRD) studies show that the number of graphene layers in nano-graphitic domains is reduced after Sn incorporation with no change in interlayer spacing. Full cells with commercial benchmark cathodes are also presented along with cost analysis of the Sn doping routes in this study to demonstrate the commercial viability of the strategy.

Introduction

Hard carbons are widely used as anode materials for Na-ion batteries because of their advantages in terms of capacity, low voltage, superior cyclability and cost-effectiveness. Most of the Na-ion batteries being developed use hard carbons as the anode material demonstrating its efficacy as an anode material.[1,2]

Hard carbon is a disordered 'non-graphitizable' carbon consisting of *randomly segregated turbostratic graphitic domains (bent, rippled, curved), micropores and heteroatom (C, H, N) bonds on the surface.*[3–6] Hard carbons are typically produced from pyrolysis of organic polymer or hydrocarbon precursors including some biomass products such as sucrose, glucose, lignin, biomass etc.[7–10] Available capacities are very much a function of precursor and processing conditions. These were first studied by Stevens et al. as anode materials for Na-ion and Li-ion batteries, and the (de)sodiation mechanisms explained by a simplified 'House of cards' model in 2000.[5] The (de)sodiation profiles of galvanostatic cycling of hard carbons consists of a sloping region (above 0.1 V) and a plateau region (below 0.1 V). The sodiation mechanism is broadly defined in three different mechanistic events – 1) *Sodium pooling in nanopores resulting in quasimetallic clusters*, 2) *intercalation in graphene layers and* 3) *Surface/defect storage*. In-situ small angle X-ray scattering (SAXS) and wide-angle X-ray scattering (WAXS) experiments by Stevens et al. in 2001 showed that lower voltage plateau sodiation consists of pooling in nanopores and the sloping region consists of Na intercalation in graphene layers, this mechanism was also observed by Komaba et al. in 2011.[5,11,12] Later, Bommier et al. suggested that Na-storage in the sloping region occurs at defect sites and the storage mechanism in the plateau region is due to intercalation in graphene layers and minor contribution by Na-ion adsorption/pooling in nanopores.[13] Through NMR studies by Stratford et al., it was proposed then that Na is more ionic in the sloping region thus it is stored at defects and/or in expanded graphene sheets, and pore-filling occurs in the lower plateau region.[14] The notion of pore filling was challenged by Qui et al. by arguing that there is no correlation between porosity (gas adsorption based porosity)

[a] *Dr. A. Tripathi, C. Murugesan, Dr. A. Naden, Dr. A. R. Armstrong, Prof. J. T. S. Irvine*
School of Chemistry
University of St Andrews
North Haugh, St Andrews, Fife, KY16 9ST (United Kingdom)
E-mail: jtsi@st-andrews.ac.uk

[b] *Dr. A. Tripathi, C. Murugesan, Dr. A. Naden, Dr. A. R. Armstrong, Prof. J. T. S. Irvine*
The Faraday Institution, Quad One
Harwell Science and Innovation Campus, OX11 0RA Didcot (United Kingdom)

[c] *Dr. P. Curran, Dr. C. M. Kavanagh*
Deregallera Ltd, Unit 2
De Clare Court Pontygwindy Industrial Estate
Caerphilly CF83 3HU (United Kingdom)

[d] *J. M. Condliffe*
Centre for Process Innovation, National Formulation Centre
The Coxon Building, John Walker Road, Sedgefield, TS21 3FE (United Kingdom)

Supporting information for this article is available on the WWW under https://doi.org/10.1002/batt.202300225

© 2023 The Authors. Batteries & Supercaps published by Wiley-VCH GmbH. This is an open access article under the terms of the Creative Commons Attribution License, which permits use, distribution and reproduction in any medium, provided the original work is properly cited.

© 2023 The Authors. Batteries & Supercaps published by Wiley-VCH GmbH

Research Article
doi.org/10.1002/batt.202300225
Chemistry Europe
European Chemical Societies Publishing

and low-voltage plateau capacity, however no SAXS measurements were performed and only open pore measurements were carried out by gas adsorption methods.[15] Alternate mechanisms have also been reported.[16,17] The exact mechanism is still debatable and there is a possibility that various events of Na absorption/pooling/intercalation occur simultaneously at various stages depending on the energy barriers arising from defects and interlayer spacing of graphene sheets.[18] Amidst the various attempts to understand the mechanism of sodium storage in hard carbons, it is important to design improved hard carbons with existing knowledge. Elongating the lower plateau region is one of the directions to improve the hard carbons. Elongating the lower voltage plateau combined with decreasing surface area not only increases the capacity but also improves the first cycle coulombic efficiency of the hard carbon.[19] We show that Sn introduction in the hard carbon can improve the plateau capacity, and the first cycle coulombic efficiency.

Heteroatom doping has been studied to both improve the electrochemistry and understand the mechanism of (de)sodiation in hard carbons.[20–22] P doped hard carbons have been extensively studied to improve the electrochemical performance of hard carbons.

NanoSn-HC composite was studied by Guo et al. for lithium-ion batteries.[23] However, the synthesis technique involved multiple steps and there was significant capacity fade. Although nano-Sn/C composites where nano-Sn is decorated in porous carbon architectures have excellent electrochemical performance, their tap density makes them an impractical choice.

In this work, a cost-effective method of Sn doping in hard carbons is presented by using simple solution impregnation. The Sn source is introduced in a porous hard carbon derived from a biowaste (B187, Deregallera Ltd.) which has been synthesized at 700 °C. The Sn precursor is impregnated at ambient conditions followed by a heat treatment at 1000 °C. Pore closures and a decrease in porosity during heat treatment at 1000 °C is expected during the synthesis. At the same time due to the presence of Sn atoms/clusters, it is hypothesized that there will be a restriction of the growth of graphitic domains. The resultant hard carbon-Sn (HC–Sn) composites show an improved capacity and first cycle coulombic efficiency. The terminology used to describe the HC–Sn composites derived from B187 hard carbon are presented as *'Temperature of heat treatment (°C) _w/w % Sn'*. The results presented in this study relate to 1000_7,1000_15, 1000_40 composites, and we also present Sn (7 %) doping in Sucrose-derived hard carbons (SDHC vs. SDHC–Sn).

Results and Discussion

XRD confirms the presence of crystalline Sn in B187 Hard-carbon derived 1000_7, 1000_15 and 1000_40 (Figure S1). Thermogravimetric analysis (TGA) in air was performed to determine the Sn content (Figure S2). Sn content was calculated assuming that SnO_2 is formed at the end of the TGA experiment.

Figure 1(a, b) shows distributed Sn in the 7 % sample with strongly cluster Sn in the 40 % sample, Figure 1(c) shows that Raman peaks from hard carbon are modified due to interaction with Sn in the 7 % sample. Figure 1(d–g) shows the STEM images of the 1000_7 sample. It clearly shows that Sn is infiltrated uniformly in the Hard Carbon with a slightly higher concentration on the surface (Figure 1b, d). As the loading of Sn is increased to 15 % and 40 %, agglomeration of micron sized Sn particles (Figure S3) was observed. Figure 2 summarizes the electrochemical performance of HC–Sn samples. First cycle desodiation capacities of 220 mAh/g, 285 mAh/g, 325 mAh/g

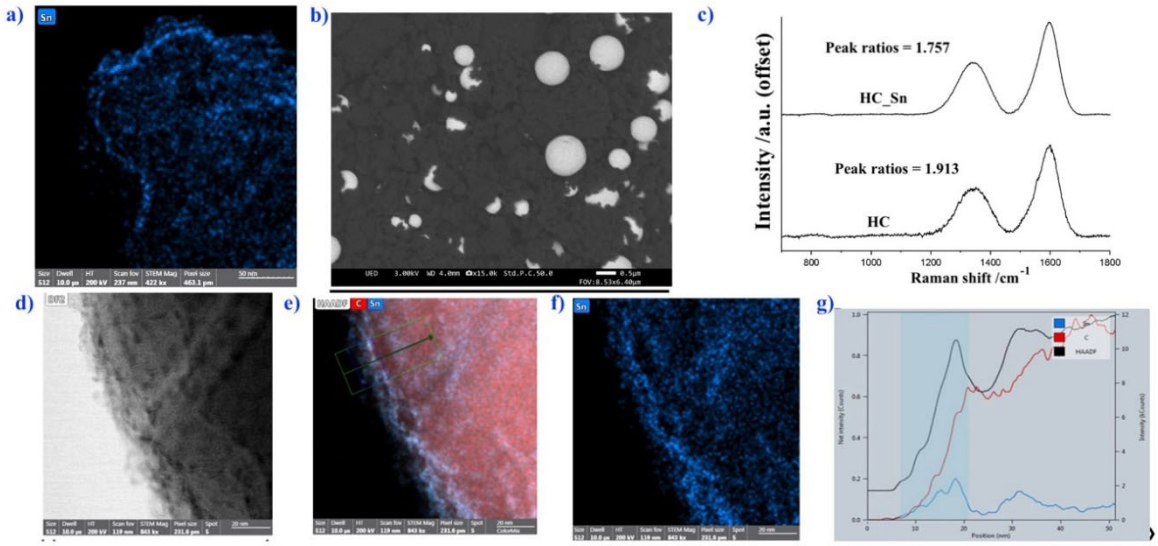

Figure 1. a) TEM EDX image of HC_Sn_1000_7. Scale bar is 50 nm. b) Comparative SEM image of HC_Sn_1000_7. The scale bar is 500 nm. c) Comparison between Raman spectra of HC_Sn_1000_0 and HC_Sn_1000_7 4 showing the changes in bond structure occur on Sn doping. d–g) show analysis through a section of HC_Sn_1000_7. d) STEM image of HC_Sn_1000_7, e) annotated STEM image with carbon and f) Sn EDX. The scale bars in (d–f) are 20 nm. g) Elemental line profile along with the line in (e).

© 2023 The Authors. Batteries & Supercaps published by Wiley-VCH GmbH

25666223, 0, Downloaded from https://chemistry-europe.onlinelibrary.wiley.com/doi/10.1002/batt.202300225 by NHS Education for Scotland NES, Edinburgh Central Office, Wiley Online Library on [18/09/2023]. See the Terms and Conditions (https://onlinelibrary.wiley.com/terms-and-conditions) on Wiley Online Library for rules of use; OA articles are governed by the applicable Creative Commons License

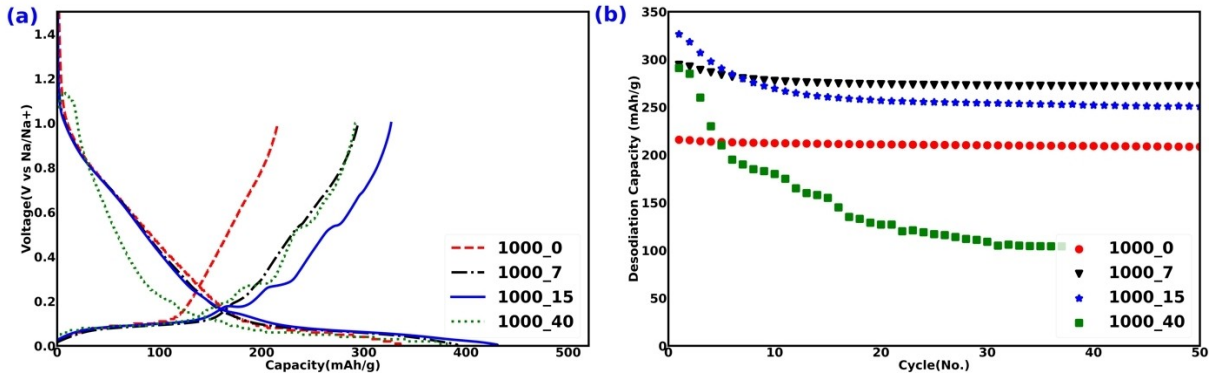

Figure 2. a) First cycle galvanostatic profiles of HC/Sn at 50 mA/g in Na-ion half cells. b) Cycling performance of HC/Sn at 50 mA/g. [Electrode composition: 95% HC/Sn, 5% CMC binder, Electrolyte: 1 M NaPF6 EC, DEC]

and 280 mAh/g were obtained for 1000_0, 1000_7, 1000_15 and 1000_40 samples respectively at 50 mA/g in Na-ion half cells (Figure 2a). There is also an improvement in first cycle coulombic efficiency (CE) from 65% for 1000_0 to 75% for 1000_7/1000_15/1000_40 samples. For the 15 and 40% samples there is clear evidence of the potentials associated with Sn alloying, whilst this is hard to discern in the 7% sample. The improvement in first cycle CE can be attributed to an increase in plateau capacity after Sn incorporation. It is well known from past studies that the plateau region is more reversible in hard carbons.[19] (De)sodiation capacity of 1000_40 sample is lower than expected as one expects an increase in capacity after increase in Sn content, this might be due to high electronic resistance of the solid-electrolyte interphase (SEI) on the Sn surface in EC:DEC electrolyte. This was confirmed by testing 1000_40 in 1 M $NaPF_6$ in Diglyme (Figure S4) in which 345 mAh/g capacity was obtained with stable cycling performance. It has been shown in recent studies that Sn cycles much better in glyme based electrolytes than for carbonate electrolytes,[24] indicating more suitable SEI formation. The cycling performance of HC/Sn samples is shown in Figure 2(b). Capacity retention of HC/Sn samples after 50 cycles at 50 mA/g was 97%, 93%, 77% and 46% for 1000_0, 1000_7, 1000_15 and 1000_40 samples respectively. The capacity retention worsens with the increase of Sn content. The following factors have been postulated to lead to poor cycling performance with increase in Sn content – a) increase in size of Sn particles through agglomeration promotes cracking of electrode architecture during cycling due to c.a. 420% volume expansion,[24,25] b) increase of Sn particles on the surface of composites with concomitant increase of electrolyte-Sn interaction leads to unstable SEI and thus poor cycling.[24,26] On further cycling the sample 1000_7 demonstrated stable cycling at 275 mAh g^{-1} up to 250 cycles, with the best long term performance (Figure S5).

Improvement in plateau capacity below 0.15 V is obtained after Sn incorporation as it is significantly improved from 93.2 mAh/g (1000_0) to 132.7 mAh/g (1000_7), this small level of Sn-doping does not seem to affect the polarisation. The capacity above 0.15 V is quite similar for 1000_7 and 1000_15 samples if one ignores the Sn related plateaux at c.a. 0.21 V, 0.25 V and 0.55 V. For the 1000_40 sample, the capacity above 0.15 V is reduced, which can be due to reduced activity of hard carbon or detrimental Sn-electrolyte interactions. It is interesting to note that plateau desodiation capacity below 0.15 V is quite similar for both 1000_7 and 1000_15 samples, see Figure 3.

An increase in plateau capacity (both sodiation and desodiation) after Sn doping may be due to *increase in closed pore size or improved Na-ion diffusivity from graphitic domains to closed pores.*[27]

In order to understand the origins of this improvement, we closely analysed powder XRD data. XRD patterns of 1000_0 and 1000_7 samples as shown in Figure 4. The *empirical R factor* which is- the ratio of 002 peak intensity and background intensity at 002 peak, was introduced by Liu et al. and it can be used to provide a relative determination of number of monolayers in graphene stacks. It has been shown by Liu et.al. that a lower value of *empirical R factor* is directly correlated with increase in plateau capacity.[4] Table 1 shows that *empirical R factor* decreases after Sn incorporation, meaning there are more monolayers in Sn doped Hard carbon. The lower plateau capacity depends on nanopore volume, nanopore size and on the ease of access of Na-ions to those nanopores. Thin graphitic

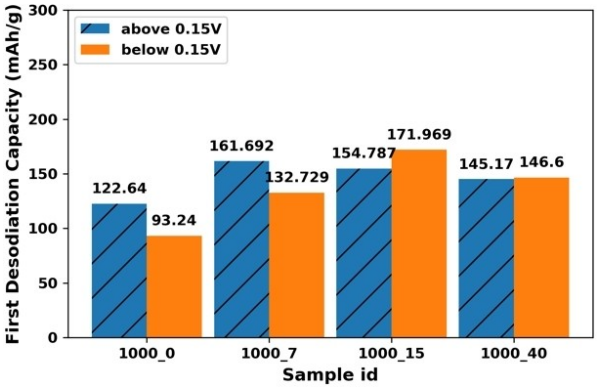

Figure 3. First desodiation capacity above and below 0.15 V of 1000_0, 1000_7, 1000_15 and 1000_40 HC/Sn samples.

© 2023 The Authors. Batteries & Supercaps published by Wiley-VCH GmbH

25666223, 0, Downloaded from https://chemistry-europe.onlinelibrary.wiley.com/doi/10.1002/batt.202300225 by NHS Education for Scotland NES, Edinburgh Central Office, Wiley Online Library on [18/09/2023]. See the Terms and Conditions (https://onlinelibrary.wiley.com/terms-and-conditions) on Wiley Online Library for rules of use; OA articles are governed by the applicable Creative Commons License

Research Article
doi.org/10.1002/batt.202300225
Chemistry Europe
European Chemical Societies Publishing

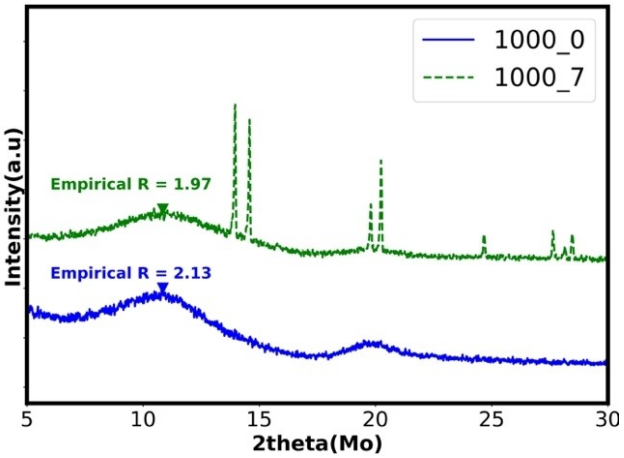

Figure 4. XRD of 1000_0 and 1000_7 samples using Mo $K\alpha_1$ radiation.

stacks or fewer graphene layers can improve the ease of access for Na-ions, thus improving both plateau capacity and initial CE.

The average number of graphene sheets in a crystallite was also calculated using the Scherrer formula, which decreases with Sn incorporation (Table 1), thus corroborating our hypothesis from *empirical R factor analysis*. BET analysis using N_2 adsorption isotherms revealed that both 1000_0 and 1000_7 consists of micropores. The specific surface areas of both 1000_0 and 1000_7 were found to be very similar (Table 1), meaning that the increment in capacity between these is not related to opening of pores.

Full cells consisting of 1000_7 (anode) and a commercially relevant cathode material were tested at 25 $mA/g_{cathode}$ (Figure 5). The full cells show an initial CE of ca. 73%, and a stable cycling performance. When the same commercial cathode is cycled against 1000_0 anode, the first cycle CE is around 64% (Figure S6). Thus, Sn incorporation has significant effect on the first cycle CE and thus energy density in a full cell system. The first cycle capacity of 275 mAh/g_{anode} is comparable to the one obtained in half cells.

In order to investigate the generalisability of this technique, we doped Sn in Sucrose-derived Hard carbon (SDHC). 7% Sn doped SDHC (SDHC–Sn) was synthesized by introducing the Sn source after the caramelization step, followed by high temperature heat treatment. Details of synthesis is given in the methods section. SDHC–Sn gives a slightly higher capacity of 280 mAh/g after 50 cycles as compared to 260 mAh/g given by SDHC after 50 cycles. The first cycle coulombic efficiency was 74% and 77% for SDHC and SDHC–Sn respectively. Cycling performance of SDHC and SDHC–Sn is shown in Figure 6(b). There is an initial loss of ca. 20 mAh/g in first 10–15 cycles of

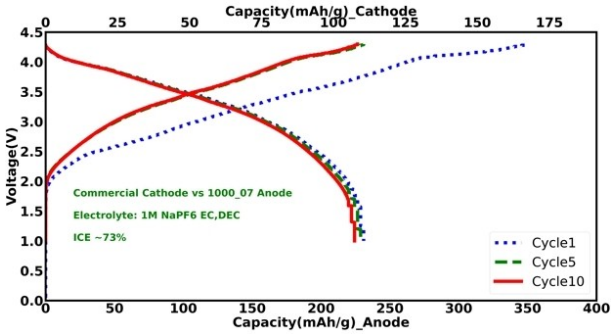

Figure 5. Full cell (commercial cathode vs. HC–Sn 1000_7) galvanostatic profiles of cycle 1, 5 and 10.

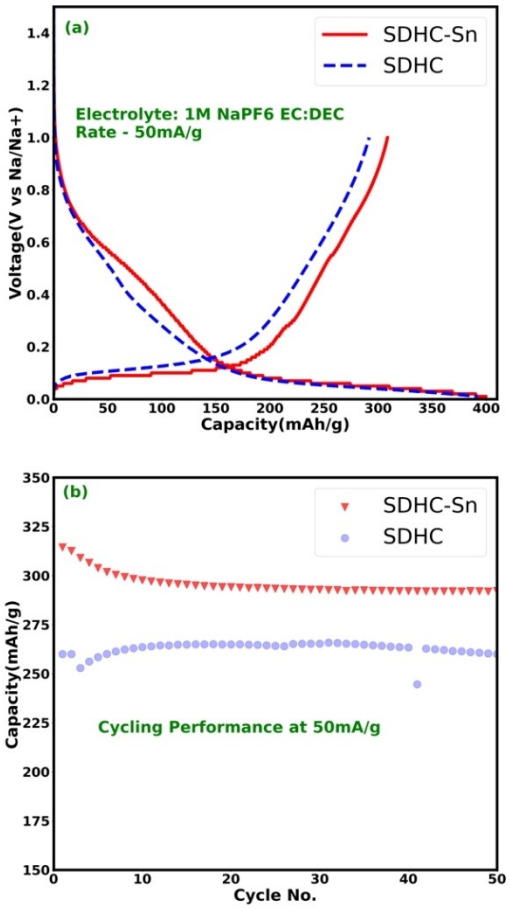

Figure 6. a) First cycle of Sucrose derived Hard carbon (SDHC) and 7% Sn doped Sucrose derived Hard carbon (SDHC–Sn) at 50 mA/g. b) Cycling performance of SDHC and SDHC-Sn.

Table 1. Determination of empirical R-factor results and BET surface area analysis.

Sample	Interlayer graphene spacing [Å]	Crystallite size [Å]	Number of stacking sheets	*R* (empirical)	BET [m^2/g]
1000_0	3.785	10.352	2.735	2.13	40
1000_7	3.749	9.058	2.416	1.97	31

© 2023 The Authors. Batteries & Supercaps published by Wiley-VCH GmbH

25666223, 0, Downloaded from https://chemistry-europe.onlinelibrary.wiley.com/doi/10.1002/batt.202300225 by NHS Education for Scotland NES, Edinburgh Central Office, Wiley Online Library on [18/09/2023]. See the Terms and Conditions (https://onlinelibrary.wiley.com/terms-and-conditions) on Wiley Online Library for rules of use; OA articles are governed by the applicable Creative Commons License

SDHC–Sn after which it stabilized. This initial loss is most likely related to the plateau related to Sn at c.a. 0.25 V and 0.50 V during desodiation. This initial loss is also observed for the 1000_7 sample (Figure 2b). Overall, the Sn doping in SDHC also leads to improved capacities and first cycle CE. This represents preliminary data on Sn doping in SDHC. The SDHC–Sn system is being optimized, and a detailed study will be published elsewhere.

It is well established in the literature that plateau capacity of hard carbon is much more reversible than for the sloping region.[7,18,19,27] The plateau capacity is related to Na-clustering/pooling in the nanopores. However, increasing the volume of nanopores is not always directly correlated with improvement in plateau capacity as one observes with hard carbons synthesized at very high temperatures (>1500 °C).[28] The interlayer spacing of graphene layers,[28] size of graphitic domains,[27] defects on the edges of graphitic layers, size of nanopores[18] also play an important role in allowing electrochemically inserted Na-ions to pool in the nanopores. We hypothesize that Sn doping creates thin graphitic layers around the nanopores, which improves the access of Na-ions to the nanopores thus improving plateau capacity and the initial CE. Empirical R factor analysis[4] also shows that after Sn doping number of monolayers of graphene is increased. The Sn particles which migrate to the surface (Figure 1), lead to initial capacity loss of HC–Sn (Figure 2b). Methods to avoid this migration or selectively remove these Sn particles can significantly improve these hard carbons.

In order to evaluate the commercial prospects of the Sn-vapour deposition process we conducted a high-level techno-economic assessment (TEA) of an industrial scale process operating at 1000 tonnes/year. Details including assumptions, flowsheet, mass balance and final economic assessment are included are presented in the Supporting Information. Figure 7 shows the B187-Sn cost as a function of wt%-Sn where the upper, base and lower cases are calculated using the dominant cost factor of $SnCl_2 \cdot 2H_2O$ price of £25.80/kg, £29.90/kg and £34/kg.

At 7 wt% Sn, the optimum fraction from this study, the cost of B187-Sn7 is estimated to be between £8.49 and £9.71, well under the £15/kg of battery grade spherical coated graphite for lithium-ion batteries.[30]

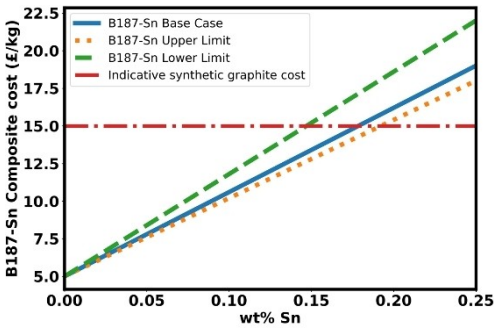

Figure 7. Estimated TEA cost of B187-Sn composite as a function of wt% Sn.

Conclusions

We hereby report Sn doping in Hard carbons - Deregallera's B187 and Sucrose derived Hard carbon. Through systematic study we conclude that 7% Sn doping is more desirable in carbonate based electrolytes as compared to 15% and 40% Sn content. Higher loading of Sn leads to poor cycling stability in carbonate-based electrolytes such as 1 M $NaPF_6$ EC-DEC. XRD analysis shows that a decrease in number of graphene layers in the graphene stacks after Sn doping leads to a better access of Na-ions to nanopores, which results in an elongation of lower voltage plateau and concomitant improvement in first cycle coulombic efficiency. Sn doping is a facile and cost-effective method to improve the first cycle coulombic efficiency of hard carbons in contrast to the expensive higher temperature heat treatments usually employed.

Experimental Section

Material synthesis

B187 1000_7, 1000_15, 1000_40

Sn doping was performed on B187 Hard carbon, which is produced from sustainable biowaste and was provided by Deregallera. 0.5 g of Hard carbon was mixed in an ethanolic solution of $SnCl_2 \cdot 2H_2O$ (Sigma Aldrich). $SnCl_2 \cdot 2H_2O$ was taken 0.1 g in excess to compensate for the vaporization loss during heat treatments. The hard carbon – $SnCl_2 \cdot 2H_2O$ in ethanol solution was dried at 30 °C, and then transferred to an alumina boat. The alumina boat containing the dried powder was heated in a tube furnace at 1000 °C under 60–100 cc/min flow rate of Argon, see Figure S7.

Sucrose derived hard carbon – Sn (SDHC, SDHC-Sn)

SDHC was synthesised by following the synthesis from a previous report.[29] In case of SDHC–Sn, after the caramelization step, the caramelized powder was mixed with ethanolic solution of $SnCl_2.2H_20$. 2 g caramelized powder was dispersed in 0.5 g $SnCl_2.2H_20$ in ethanol solution. The following steps were the same as that of 1000_7, 1000_15 and 1000_40 samples, except that the final heat treatment was carried out at 1100 °C instead of 1000 °C.

Electrochemical characterization

Slurries of 95% active material (hard carbon/hard carbon-Sn) and 5% Carboxy Methyl Cellulose-Sodium salt was prepared in deionized water. Slurries were cast on Aluminium foil (Advent Ltd.) using a doctor blade with 200 μm gap. The cast was dried at 80 °C in ambient air. 1.5 cm^2 disks were punched out after the drying process. The electrode disks were dried overnight at 80 °C, under vacuum in the antechamber of an MBraun Glovebox. 2032 type cell assembly were performed inside an Argon filled ($H_2O < 0.1$ ppm, $O_2 < 0.1$ ppm) glovebox (MBraun).

Na metal (Sigma Aldrich) was used as the counter electrode for Na-ion half cells. In case of full cells, commercial cathode material was used as the cathode material. Whatman Glass fibre separators (GE) were used for all cells. Electrolytes used in this study were- 1 M $NaPF_6$ in EC (ethylene carbonate) DEC (diethyl carbonate (1:1 v/v)

© 2023 The Authors. Batteries & Supercaps published by Wiley-VCH GmbH

25666223, 0, Downloaded from https://chemistry-europe.onlinelibrary.wiley.com/doi/10.1002/batt.202300225 by NHS Education for Scotland NES, Edinburgh Central Office, Wiley Online Library on [18/09/2023]. See the Terms and Conditions (https://onlinelibrary.wiley.com/terms-and-conditions) on Wiley Online Library for rules of use; OA articles are governed by the applicable Creative Commons License

supplied by Kishida Chemical Co., Ltd. and 1 M $NaPF_6$ (Sigma Aldrich) in diglyme (Alfa Aesar).

Galvanostatic cycling was performed on a Neware BTS4000 cycler.

Material characterization

XRD was carried out in 0.5 mm capillaries on Stoe STADIP diffractometer fitted with a Mythen linear detector (Mo $K\alpha_1$ radiation, $\lambda = 0.7093$ Å). TEM images were taken on Titan Themis which is equipped with EDS and EELS imaging. N_2 adsorption/desorption BET measurements were performed on samples degassed overnight at 150 °C on a Tristar instrument.

Acknowledgements

We would like to thank the Faraday Institution NEXGENNA project (FIRG018) and EPSRC (EP/L017008/1, EP/T019298/1, and EP/R023751/1) for support. The research data supporting this publication can be accessed at https://doi.org/10.17630/0563fb0d-1cd2-4fe8-b077-66421f5125ad

Conflict of Interests

The authors declare no conflict of interest.

Data Availability Statement

The data will be made available on Pure after manuscript acceptance and before publication

Keywords: anodes · cost analysis · energy density · hard carbon · Na-ion batteries

[1] A. Rudola, A. J. R. Rennie, R. Heap, S. S. Meysami, A. Lowbridge, F. Mazzali, R. Sayers, C. J. Wright, J. Barker, *J. Mater. Chem. A* **2021**, *9*, 8279–8302.
[2] A. Bauer, J. Song, S. Vail, W. Pan, J. Barker, Y. Lu, *Adv. Energy Mater.* **2018**, *8*, 1702869.
[3] E. Buiel, A. George, J. Dahn, *Carbon* **1999**, *37*, 1399–1407.
[4] Y. Liu, J. Xue, T. Zheng, J. Dahn, *Carbon* **1996**, *34*, 193–200.ss.
[5] D. Stevens, J. Dahn, *J. Electrochem. Soc.* **2000**, *147*, 1271.
[6] P. Zhou, R. Lee, A. Claye, J. E. Fischer, *Carbon* **1998**, *36*, 1777–1781.
[7] H. Yamamoto, S. Muratsubaki, K. Kubota, M. Fukunishi, H. Watanabe, J. Kim, S. Komaba, *J. Mater. Chem. A* **2018**, *6*, 16844–16848.
[8] Y. Li, Y. S. Hu, M. M. Titirici, L. Chen, X. Huang, *Adv. Energy Mater.* **2016**, *6*, 1600659.
[9] N. Zhang, Q. Liu, W. Chen, M. Wan, X. Li, L. Wang, L. Xue, W. Zhang, *J. Power Sources* **2018**, *378*, 331–337.
[10] Y. Zheng, Y. Wang, Y. Lu, Y.-S. Hu, J. Li, *Nano Energy* **2017**, *39*, 489–498.
[11] D. Stevens, J. Dahn, *J. Electrochem. Soc.* **2001**, *148*, A803.
[12] S. Komaba, W. Murata, T. Ishikawa, N. Yabuuchi, T. Ozeki, T. Nakayama, A. Ogata, K. Gotoh, K. Fujiwara, *Adv. Funct. Mater.* **2011**, *21*, 3859–3867.
[13] C. Bommier, T. W. Surta, M. Dolgos, X. Ji, *Nano Lett.* **2015**, *15*, 5888–5892.
[14] J. M. Stratford, P. K. Allan, O. Pecher, P. A. Chater, C. P. Grey, *Chem. Commun.* **2016**, *52*, 12430–12433.
[15] S. Qiu, L. Xiao, M. L. Sushko, K. S. Han, Y. Shao, M. Yan, X. Liang, L. Mai, J. Feng, Y. Cao, *Adv. Energy Mater.* **2017**, *7*, 1700403.
[16] N. Sun, Z. Guan, Y. Liu, Y. Cao, Q. Zhu, H. Liu, Z. Wang, P. Zhang, B. Xu, *Adv. Energy Mater.* **2019**, *9*, 1901351.
[17] S. Alvin, D. Yoon, C. Chandra, H. S. Cahyadi, J.-H. Park, W. Chang, K. Y. Chung, J. Kim, *Carbon* **2019**, *145*, 67–81.
[18] H. Au, H. Alptekin, A. C. Jensen, E. Olsson, C. A. O'Keefe, T. Smith, M. Crespo-Ribadeneyra, T. F. Headen, C. P. Grey, Q. Cai, *Energy Environ. Sci.* **2020**, *13*, 3469–3479.
[19] Y. Morikawa, S. i. Nishimura, R. i. Hashimoto, M. Ohnuma, A. Yamada, *Adv. Energy Mater.* **2020**, *10*, 1903176.
[20] P. Bai, Y. He, X. Zou, X. Zhao, P. Xiong, Y. Xu, *Adv. Energy Mater.* **2018**, *8*, 1703217.
[21] Z. Li, C. Bommier, Z. S. Chong, Z. Jian, T. W. Surta, X. Wang, Z. Xing, J. C. Neuefeind, W. F. Stickle, M. Dolgos, *Adv. Energy Mater.* **2017**, *7*, 1602894.
[22] Y. Qian, S. Jiang, Y. Li, Z. Yi, J. Zhou, T. Li, Y. Han, Y. Wang, J. Tian, N. Lin, *Adv. Energy Mater.* **2019**, *9*, 1901676.
[23] B. Guo, J. Shu, K. Tang, Y. Bai, Z. Wang, L. Chen, *J. Power Sources* **2008**, *177*, 205–210.
[24] B. Zhang, G. Rousse, D. Foix, R. Dugas, D. A. D. Corte, J. M. Tarascon, *Adv. Mater.* **2016**, *28*, 9824–9830.
[25] J. W. Wang, X. H. Liu, S. X. Mao, J. Y. Huang, *Nano Lett.* **2012**, *12*, 5897–5902.
[26] L. D. Ellis, T. D. Hatchard, M. N. Obrovac, *J. Electrochem. Soc.* **2012**, *159*, A1801.
[27] A. Kamiyama, K. Kubota, D. Igarashi, Y. Youn, Y. Tateyama, H. Ando, K. Gotoh, S. Komaba, *Angew. Chem. Int. Ed.* **2021**, *60*, 5114–5120.
[28] H. Alptekin, H. Au, A. C. Jensen, E. Olsson, M. Goktas, T. F. Headen, P. Adelhelm, Q. Cai, A. J. Drew, M.-M. Titirici, *ACS Appl. Energ. Mater.* **2020**, *3*, 9918–9927.
[29] W. Xing, J. Xue, J. Dahn, *J. Electrochem. Soc.* **1996**, *143*, 3046.
[30] https://westwaterresources.net/minerals-portfolio/graphite-market/.
[31] http://www.marketindex.com.au/news/graphite-from-evolution-energy-minerals-produces-super-premium-class-of.

Manuscript received: August 8, 2023
Revised manuscript received: August 17, 2023
Accepted manuscript online: August 21, 2023
Version of record online: ■■, ■■

© 2023 The Authors. Batteries & Supercaps published by Wiley-VCH GmbH

25666223, 0, Downloaded from https://chemistry-europe.onlinelibrary.wiley.com/doi/10.1002/batt.202300225 by NHS Education for Scotland NES, Edinburgh Central Office, Wiley Online Library on [18/09/2023]. See the Terms and Conditions (https://onlinelibrary.wiley.com/terms-and-conditions) on Wiley Online Library for rules of use; OA articles are governed by the applicable Creative Commons License

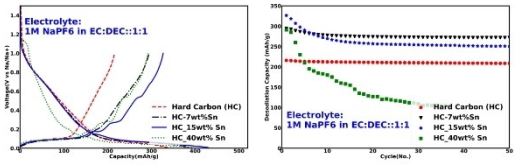

Cost effective anode: Improvements in hard carbon negatives achieved through Sn doping with improvement in electrochemical performance. Specifically, improvement in plateau region of hard carbon is observed with no compromise on initial coulombic efficiency.

*Dr. A. Tripathi, C. Murugesan, Dr. A. Naden, Dr. P. Curran, Dr. C. M. Kavanagh, J. M. Condliffe, Dr. A. R. Armstrong, Prof. J. T. S. Irvine**

1 – 7

Investigations into Improved Electrochemical Performance of Sn Doped Hard Carbons as Negatives for Sodium-Ion Batteries

25666223, 0, Downloaded from https://chemistry-europe.onlinelibrary.wiley.com/doi/10.1002/batt.202300225 by NHS Education for Scotland NES, Edinburgh Central Office, Wiley Online Library on [18/09/2023]. See the Terms and Conditions (https://onlinelibrary.wiley.com/terms-and-conditions) on Wiley Online Library for rules of use; OA articles are governed by the applicable Creative Commons License